encit 2020

ABCM
Associação Brasileira de Engenharia e Ciências Mecânicas

18th Brazilian Congress of Thermal Sciences and Engineering
November 16–20, 2020 (Online)

ENC-2020-0617
NUMERICAL AERODYNAMIC SIMULATION OF AN ARTILLERY PROJECTILE WITH A BASE BLEED SYSTEM

Rachel Lucena[1]
Norberto Mangiavacchi
José da Rocha Miranda Pontes
Daniel José Nahid Mansur Chalhub
Gil Roberto V. Pinheiro
Wallace Ramos Rosendo da Silva
Leib de Andrade Neubarth
Rio de Janeiro State University, Rio de Janeiro, RJ, Brazil
rachel.lucena@gmail.com, norberto.mangiavacchi@eng.uerj.br, pontes.jose@gmail.com, daniel.chalhub@eng.uerj.br
gilpinheiro@eng.uerj.br,wrosendoeng@gmail.com,leib999@yahoo.com.br

Maurício Ferrapontoff Lemos
Brazilian Navy Research Institute (IPqM), Rio de Janeiro, Brazil
engmlemos@gmail.com

Laurílio José da Silva Júnior
Empresa Gerencial de Projetos Navais (EMGEPRON), Rio de Janeiro, Brazil[1]
laurilio.jr@gmail.com

Abstract. *A flying object such as a munition projectile has a limited range in part due to aerodynamic drag. One way to increase rear pressure is through the insertion of the combustion products generated by the burning of a propellant, by the so called Base Bleed system. A munition with a Base Bleed system is normally called as an "extended range" munition. There are no models or commercially available software to be used to predict a specific propellant formulation which will deliver the desired performance - the only way is through a real test in a shooting range, which demands a costly logistics and great risks. In this work, we investigate the supersonic flow around an artillery projectile to relate the influence of the base bleed system on the drag coefficient using CFD. We consider a supersonic airflow on two-dimensional axisymmetric domain and we solve the governing equations by OpenFOAM software. After the tests, we found/confirm that there is an optimum value for the gas flow velocity from the base bleed unit which produces the larger drag reduction.*

Keywords: *artillery munition, base pressure, base bleed, drag coefficient, CFD*

1. INTRODUCTION

A flying object such as a munition projectile has limited range in part due to aerodynamic drag, where the main resistance is caused by the low pressure region formed in the rear part of the projectile, the so called "base drag". One way to increase rear pressure is through the insertion of combustion products generated by the burning of a propellant, a system called Base Bleed (BB) (Belaidouni *et al.*, 2016; Bournot *et al.*, 2006; Lemos *et al.*, 2013; Xue and Yu, 2016; Zhang *et al.*, 2017; Mathur and Dutton, 1996; Lee and Kim, 2006).

A munition with a BB system is normally called as an "extended range" (ER) munition. The design of a propellant to be used in such system is not simple and there are few manufacturers around the globe (Börngen and Hahn, 1988; Costa and Barboza, 2000; Gauchoux *et al.*, 1988; Gunners *et al.*, 1988; Haugen *et al.*, 1988; Lemos *et al.*, 2017). Hence, there are no models or commercially available software to be used to predict a specific propellant formulation which will deliver the desired performance - the only way is through a real test in a shooting range, which demands a costly logistics and great risks. Therefore, it is remarkably interesting to develop lab scale tests and models to predict the performance of extended range projectiles, without the need of several real shooting tests. For that, a recently joint research group formed by the Brazilian Navy together with the Rio de Janeiro State University endeavor in a research to develop a network of models and algorithms that might allow a good prediction of the performance of extended range munitions by using simple lab scale test bench.

Some authors have performed CFD calculations to predict and evaluate the base drag of artillery projectiles using

base bleed technology. Regodić *et al.* (2013) developed a numerical model to predict of axial aerodynamic coefficient reduction using the BB system which takes account the gas generator mass flow prediction, base drag reduction caused by mass injected into the wake region and the geometry of propellant grain. They confirm that the extend range of artillery projectile is proportional to reduction of axial aerodynamic coefficient.

Dali and Jaramaz (2019) have studied a way to effectively control and optimize the base flow for base drag reduction, using an adequate (CFD) software. The authors concluded that for the projectiles with various propellant types, which the combustion temperatures change in small interval and seeing the CFD results with H_2O and HCl injection, the molecular weight has an exceptional role in terms of drag reduction.

The total drag of projectiles can be composed of two main components: forebody drag (skin friction and pressure drag) and base drag. For Mach number equal to 0.9, the base drag is approximately 50% of the total amount of drag (Sahu *et al.*, 1985). In this work, we investigated the supersonic flow around an artillery projectile with $4.5-$inch caliber to relate the influence of the BB system on the drag coefficient with CFD calculations. To achieve this, we have studied the variation of the velocity and temperature in the orifice of the bleed gases. We considered different values to Mach number at BB unit, including zero velocity which means without BB system.

2. MATHEMATICAL MODEL AND NUMERICAL METHOD

We consider airflow on two-dimensional axisymmetric domain, this approach is considered because is a powerful technique to reduce the computational cost. The fluid (air) is considered ideal gas ($p = \rho RT$). Hence, the governing equations are described as follows:

$$\frac{\partial \rho}{\partial t} + \nabla \cdot (\rho \mathbf{u}) = 0 \tag{1}$$

$$\frac{\partial \rho \mathbf{u}}{\partial t} + \nabla \cdot (\rho \mathbf{u}\mathbf{u}) - \nabla \cdot \mu(\nabla \mathbf{u} + \nabla \mathbf{u}^T) = -\nabla p \tag{2}$$

$$\frac{\partial \rho e}{\partial t} + \nabla \cdot (\rho \mathbf{u} e) - \nabla \cdot \left(\frac{k}{C_v}\right) \nabla e = p \nabla \cdot \mathbf{u} \tag{3}$$

where Eqs. 1 to 3 are, respectively, the mass continuity equation, momentum equation for Newtonian fluid and energy equation for fluid (ignoring some viscous terms), $e = C_v T$, with Fourier's Law $q = -k\nabla T$.

2.1 Parameters

The evaluation of the simulations results is performed by calculating the drag coefficient, C_D, and the mass injection parameter, I. Thus the drag coefficient is given by:

$$C_D = \frac{2F_D}{\rho_\infty U_\infty^2 A_b} \tag{4}$$

where the F_D is the drag force magnitude, ρ_∞ and U_∞ are the density and velocity of free-stream magnitude, respectively, and A_b is the base area of the projectile.

By imposing the velocity and temperature, we have calculated the injected mass flow rate $\dot{m}_{BB}$ of hot gas in the orifice at the rear part of the BB unit (see red highlight in Fig. 1). Therefore, the mass injection parameter, I, can be determined as the ratio of the injected mass flow rate and the free-stream mass flow passing through the base area of the projectile, using the Eq. 5.

$$I = \frac{\dot{m}_{BB}}{\rho_\infty U_\infty A_b} \tag{5}$$

where the $\dot{m}_{BB}$ is the mass flux through the orifice of BB unit.

2.2 Boundary and initial conditions

The boundary conditions on the domain are: at the left of the domain (inlet) the prescribed values of velocity $U = M = 2.0$, pressure $p = 1$, and temperature $T = 1$ are imposed. These values were normalized by the speed of sound in the gas, resulting in the velocities directly equivalent to the Mach number, and free-stream pressure and temperature conditions. We impose zero flux for U and T at the right (outlet) and the upper boundaries, for the pressure on the upper and right sides was considered a wave transmissive outflow condition. Pressure and temperature on the contour of projectile we employ zero flow, and no-slip condition for velocity. For the base of BB unit we impose: $\nabla p = 0$, for the temperature we impose a range from $T = 1.00$ (15°C) and $T = 7.20$ to 8.59, which means 1800°C to 2200°C; for the velocity we also prescribe several Mach numbers at the subsonic flow, $M_{BB} = 0.0 - 0.9$ (see Fig. 1).

Initial conditions for the simulations are uniform free-stream conditions in the whole domain.

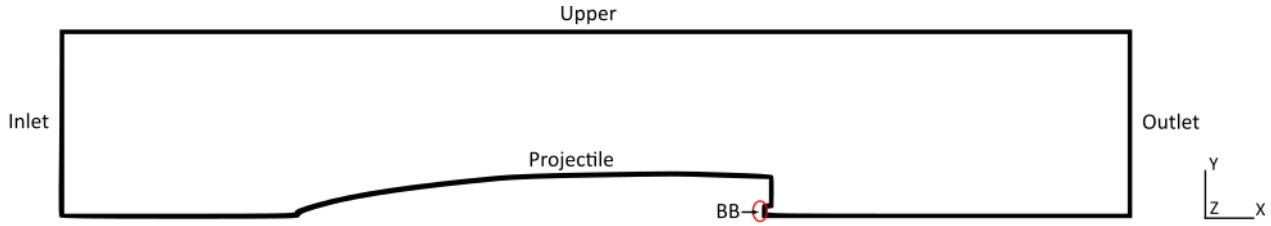

Figure 1. Schematic diagram of the numerical domain.

2.3 Numerical approach

The solution of the equations (1)-(3) is given by OpenFOAM v1912 software, using the sonicFoam solver. OpenFOAM uses the finite volume method and the unstructured finite volume mesh, produced employing Gmsh mesh generator, is showed in Fig. 2. It can be seen a region of refined mesh was used close to the projectile surface (yellow) to resolve the boundary layer gradients, as well as the flow details of the base recirculation, and a less refined mesh (green) far from the projectile.

The computational grid size was 28,551 nodes and 84,677 volumes. The time interval used was $\Delta t = 1.0 \times 10^{-5}$. Considering the normalized end time $t = 1.5$, the execution time to serial computing (only one processor) was estimated in 20h, however, when we used parallel computation (12 processors) the time execution was reduced to 1.5h. The Sutherland's method was employed to calculate the viscosity, μ, as a function of the temperature, T, where the coefficient and temperature of Sutherland were specified according to the the normalized process applied.

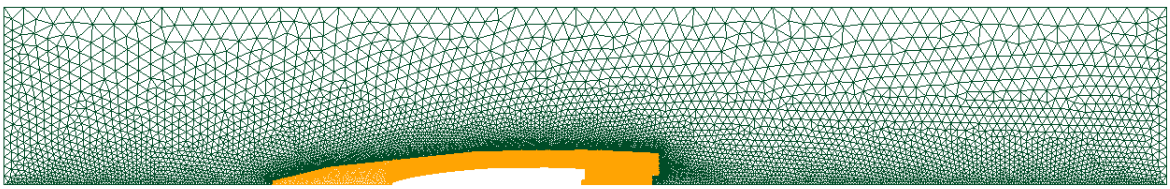

Figure 2. Bidimensional axisymmetric computational grid.

3. NUMERICAL RESULTS AND DISCUSSION

In this section, we present the results obtained considering Reynolds number $\mathrm{Re} = 3.68 \times 10^6$ and Mach number $M = 2.0$. The flow velocity is normalized by the free-stream sound speed. Figures 3-5 show three cases for different values of gas flow and temperature in the orifice of the BB.

3.1 Velocity and pressure field

Figure 3(a) shows the velocity field with a inert BB system and Figs. 4 and 5(a) show the velocity fields considering two cases with active BB system, both with $T = 8.59$ at BB unit and with $M_{BB} = 0.3$ and $M_{BB} = 0.8$ as the gas flow velocity. It can be seen that flow at the forebody of the munition is essentially not altered by the BB system. However, for the case of active BB the compression waves zone near the rear part of the projectile is attenuated, hence the thickness of wake zone is greater.

Figures 3-5(b) show the stream-lines, with colors indicating the pressure distribution. In the case of non-active BB appears a large recirculation, associated to a low pressure region. In the case with active BB, we have two different but similar results. In the case with the lowest gas flow velocity ($M_{BB} = 0.3$), we have apparently a single recirculation region, but close to the axis of symmetry it is possible to observe that there is a beginning of the formation of a second recirculation zone (see Fig. 4(b)).

In the case with the highest velocity presented of the escape of gases ($M_{BB} = 0.8$), there are three separate recirculations, but both the primary (left-bottom), secondary (right) and tertiary (left-top) circulations are much weaker than the single recirculation, and the pressure at the base of projectile does not drop as much as the previous case, as can be seen in Fig. 5(b). In particular, the minimum pressure in the recirculation, in case with inert BB is 0.319, compared to 0.458 in the case of active BB (see Figs. 3(b) and 5(b)).

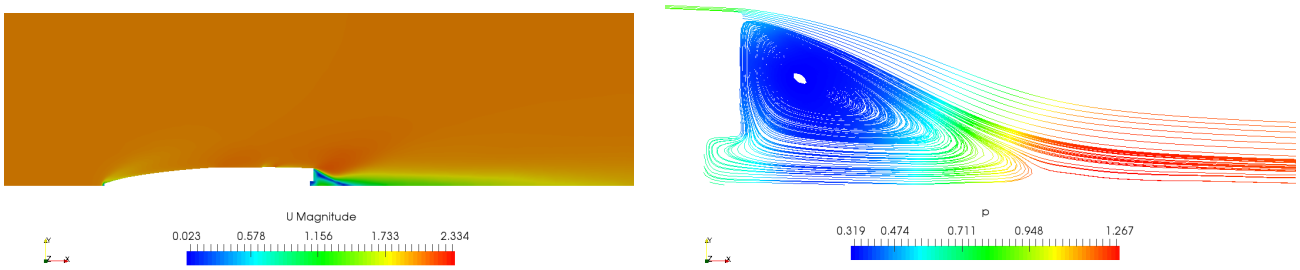

(a) (b)

Figure 3. Results for the problem considering a flow of Mach 2.0 and no BB system: (a) Velocity field; (b) Stream lines from the base of the projectile (zoom in), colored by values of the pressure, both in $t = 1.5$.

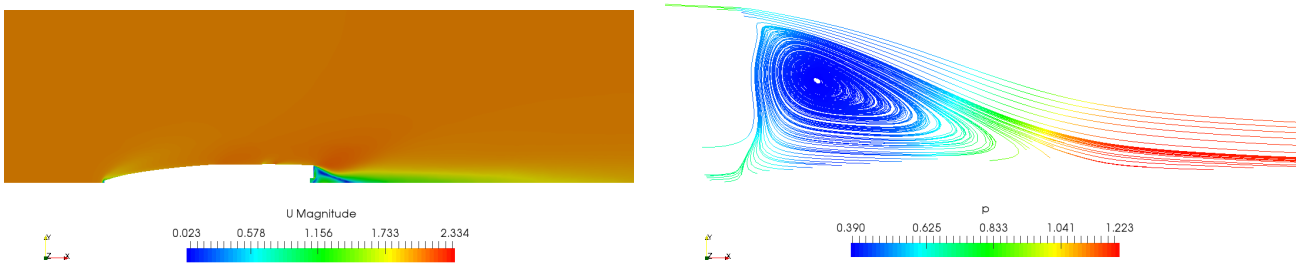

(a) (b)

Figure 4. Results for the problem considering a flow of Mach 2.0, the velocity and temperature in the BB system equal to Mach 0.3 and $T = 8.59$, respectively: (a) Velocity field; (b) Stream lines from the base of the projectile (zoom in), colored by values of the pressure, both in $t = 1.5$.

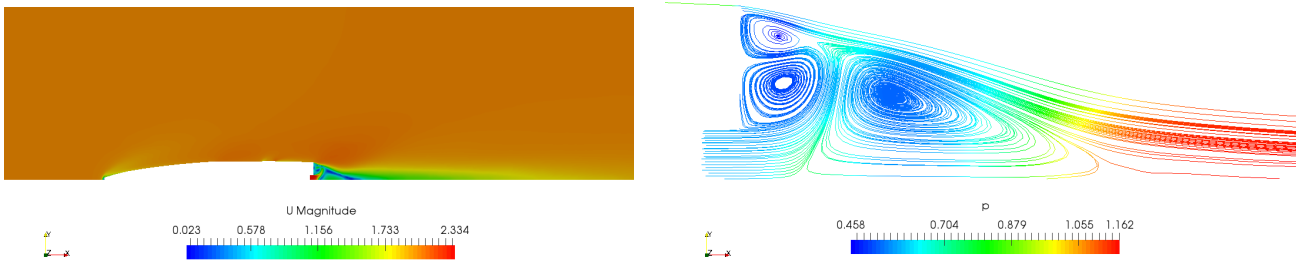

(a) (b)

Figure 5. Results for the problem considering a flow of Mach 2.0, the velocity and temperature in the BB system equal to Mach 0.8 and $T = 8.59$, respectively: (a) Velocity field; (b) Stream lines from the base of the projectile (zoom in), colored by values of the pressure, both in $t = 1.5$.

3.2 Drag coefficient and injection parameter

The drag coefficients for the five simulations performed were calculated using Eq. 4 and are shown in Fig. 6. Although the results are still preliminary, they show the expected behaviour for the BB effect, such as, for Mach = 0.0 (without BB) the drag coefficient is higher, for Mach = 0.8 the drag coefficient is the smallest and, for the case of BB Mach number equal to 0.3 we have an intermediate value for the drag coefficient.

The effect of the gas flow temperature is near negligible. When the temperature increases in the BB unit, the drag coefficient decreases only very slightly, as it can be seen in Fig. 6 in the cases with $T = 7.20$ and $T = 8.59$, considering the gas flow velocity equal to $M_{BB} = 0.3$ (red curves with and without symbols).

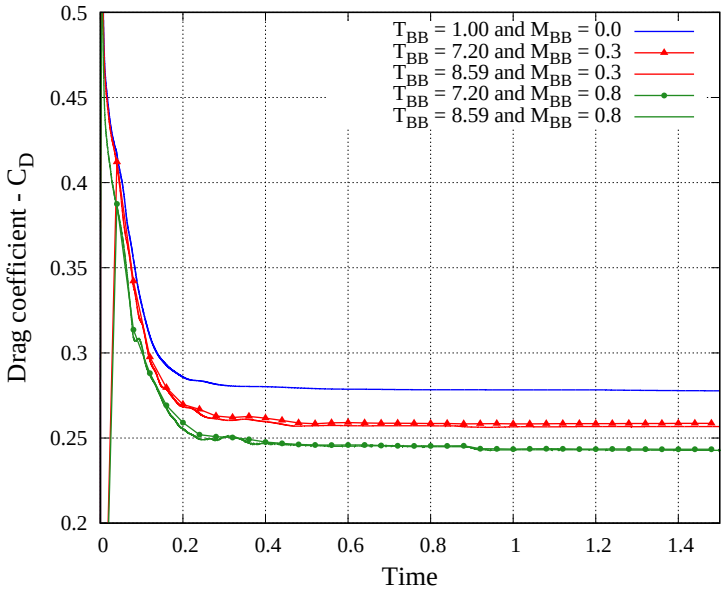

Figure 6. Drag coefficient for the five runs considering the effect of BB and three values of temperature as $M_{BB} = 0.0, 0.3$ and 0.8 up to steady-state ($t = 1.5$).

As defined in Eq. 5, we present the injection parameter results for six cases performed considering the effect of active BB system, as can be seen in Fig. 7(a). Each case considers three values of temperature: $T = 7.20, 7.89$ and 8.59, with the velocity of gases exit from the orifice of BB unit equal to $M_{BB} = 0.3$ and 0.8. From these results we can observe that the velocity is less significant than the temperature of exhaust gases, although when we have measured the injection parameter for only one temperature we observed that for high velocities we have bigger injection results (see Fig. 7(b)). We also observed that for lower temperatures the injection parameter is higher, which means that the ratio of the injected mass flow rate and the free-stream mass flow passing through the base area of the projectile is small to higher temperatures.

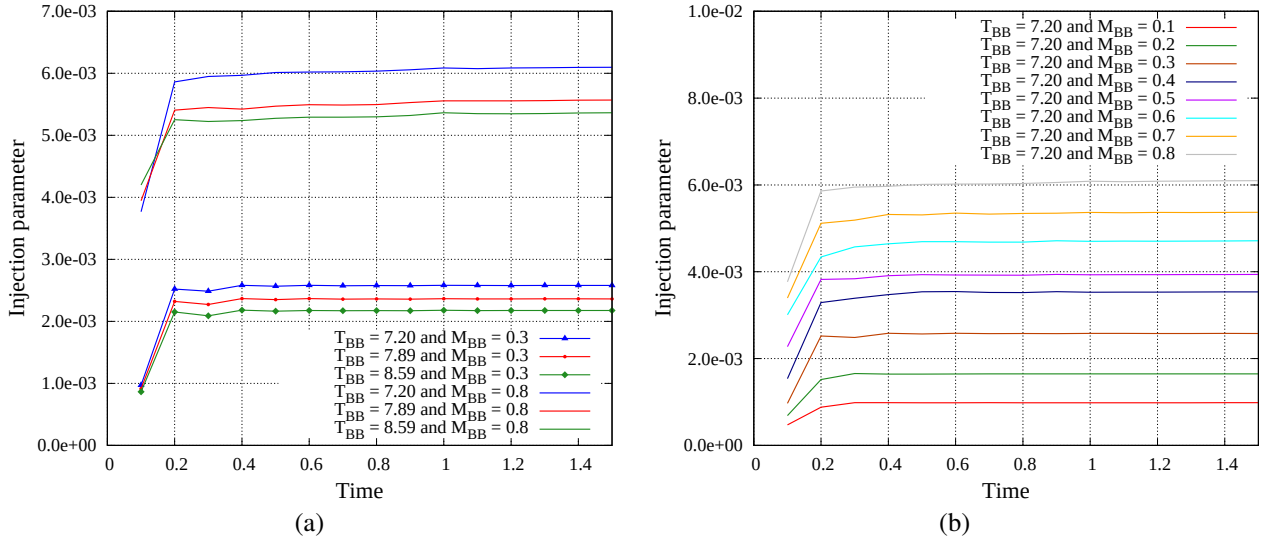

(a) (b)

Figure 7. Injection parameter up to steady-state ($t = 1.5$). (a) Injection parameter for six runs considering the effect of active BB system, cases consider three values of temperature ($T = 7.20, 7.89$ and 8.59) with $M_{BB} = 0.3$ and 0.8 for each temperature; (b) Injection parameter for $T = 7.20$ for a range from $M_{BB} = 0.1$ to 0.8.

In this work, we have studied a variation of the velocity of gases escape of BB system considering the transonic regime, aiming to relate the influence of the base bleed system on the drag coefficient. Thus, we have also performed simulations for a range of temperatures $T = 7.20$, 7.55, 7.89, 8.24 and 8.59, these values were normalized by the speed of sound of gas and are equivalents to $T = 1800$, 1900, 2000, 2100 and $2200°C$. All these results can be observed in a plot that relates the drag coefficient and the injection parameter, as showed in Fig. 8. This figure shows the influence of temperature of escape of gases from the BB unit on the drag coefficient and the mass injection parameter. The smaller the mass injection parameter, the smaller is the amount of mass flow injected at the base of projectile (Sahu *et al.*, 1985). Therefore, Fig. 8 shows that the lower the temperature of the gas flow, the higher the amount of mass injected at the base

of projectile.

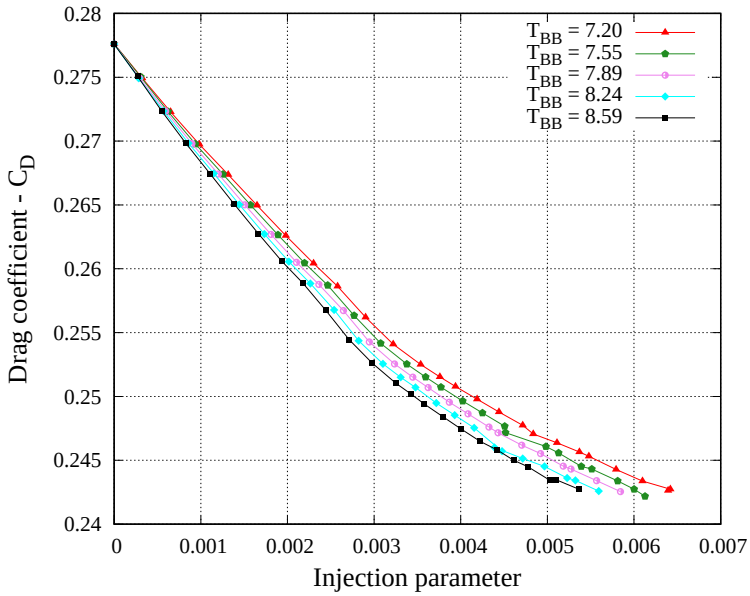

Figure 8. Drag coefficient as a function of the injection parameter for five cases with different temperatures of gases exit. Each curve was obtained from a velocity range from $M_{BB} = 0$ to 0.9.

4. CONCLUSIONS

In this work, we performed numerical simulations of the supersonic flow around a $4.5-$inch caliber projectile. The Base Bleed system is studied, varying the velocities and temperatures of the gas flow.

The decrease of the recirculation region in the wake zone indicates the BB effect, as can be seen in the literature (Mathur and Dutton, 1996; Xue and Yu, 2016), that results in the reduction of the drag coefficient. It can be observed that there is an optimum value for the speed of the gas exit due to the burning of the propellant grain in transonic flow. The results obtained by the simulation present a good agreement with results from the literature review.

In this study we have imposed some parameters (velocity and temperature) and then we get to the mass flow through the BB boundary and the respective injection parameter. It can be affirmed that the grain propellant burning products and characteristics has a particular role in terms of determining the drag coefficient, and, consequently, in drag reduction, in agreement with (Dali and Jaramaz, 2019).

Results with a range of free-stream Mach numbers, Reynolds numbers and BB Mach numbers, relevant to the computation of projectile trajectory, will be performed in future works.

5. ACKNOWLEDGEMENTS

The authors would like to acknowledge financial support from FAPERJ, CNPq, CAPES, EMGEPRON, and UERJ.

6. REFERENCES

Belaidouni, H., Živkovi ć, S. and Samardži ć, M., 2016. "Numerical simulations in obtaining drag reduction for projectile with base bleed". *Scientific Technical Review*, Vol. 66, No. 2, pp. 36–42.

Börngen, L. and Hahn, U., 1988. "Structure and ballistic properties of the rheinmetall RH 49 base bleed projectile". *Base Bleed First International Symposium on Special Topics in Chemical Propulsion*. doi: 10.1615/IntJEnergeticMaterialsChemProp.v1.i1-6.170.

Bournot, H., Daniel, E. and Cayzac, R., 2006. "Improvements of the base bleed effect using reactive particles". *International Journal of Thermal Sciences*, Vol. 45, No. 11, pp. 1052–1065.

Costa, A. and Barboza, M., 2000. "Desenvolvimento de "sistemas base bleed" para granadas he de obuseiros 155 mm". Technical report, Instituto Militar de Engenharia.

Dali, M.A. and Jaramaz, S., 2019. "Optimization of artillery projectiles base drag reduction using hot base flow". *Thermal Science*, Vol. 23, No. 1, pp. 353–364.

Gauchoux, J., Coupez, D. and Lecoustre, M., 1988. "Base bleed solid propellant – properties and processability for industrial solid propellant". *Base Bleed First International Symposium on Special Topics in Chemical Propulsion*.

Gunners, N.E., Andersson, K. and Nilsson, Y., 1988. "Testing of parts and complete units of the swedish base bleed

system". *International Journal of Thermal Sciences*.

Haugen, S., Melby, K. and Oppegåard, A., 1988. "Development and production of base bleed grain for 155 mm rounds". *International Journal of Thermal Sciences*.

Lee, Y.K. and Kim, H.D., 2006. "Optimization of mass bleed control for base drag reduction of supersonic flight bodies". *J. of Thermal Science*, Vol. 15, No. 3, pp. 206–212.

Lemos, M., Amaral, P.S.T., dos Santos, R., Miceli, A., Mattos, E.C. and Dutra, R.C.L., 2013. "Caracterização de propelente de munição de alcance estendido por análise térmica e FT-IR". *PESQUISA NAVAL (SDM)*, Vol. 25, pp. 70–75.

Lemos, M., Amaral, P., Miceli, A., Silva-Junior, L. and Souza, E., 2017. "Development of national base bleed propellant grain applied for extended range ammunition". *PESQUISA NAVAL (SDM)*, Vol. 29, pp. 49–58.

Mathur, T. and Dutton, J.C., 1996. "Velocity and turbulence measurements in a supersonic base flow with mass bleed". *AIAA JOURNAL*, Vol. 34, No. 6, pp. 1153–1159.

Regodić, D., Jevremović, A. and Jerković, D., 2013. "The prediction of axial aerodynamic coefficient reduction using base bleed". *Aerospace Science and Technology*, Vol. 31, No. 1, pp. 24–29.

Sahu, J., Nietubicz, C.J. and Steger, J.L., 1985. "Navier-Stokes computations of projectile base flow ar transonic speeds with and without base injection". *AIAA JOURNAL*, Vol. 23, No. 9, pp. 1348–1355.

Xue, X. and Yu, Y., 2016. "An improvement of the base bleed unit on base drag reduction and heat energy addition as well as mass addition". *Applied Thermal Engineering*, Vol. 109, pp. 238–250.

Zhang, L., Tian, R. and Zhang, Z., 2017. "Burning rate of ap/htpb base-bleed composite propellant under free ambient pressure". *Aerospace Science and Technology*.

7. RESPONSIBILITY NOTICE

The authors are solely responsible for the printed material included in this paper.